ARTICLE

Spectral Tuning of Organic Nanocolloids by Controlled Molecular Interactions

Christopher M. Spillmann,* Jawad Naciri,* George P. Anderson, Mu-San Chen, and Banahalli R. Ratna*

Center for Bio/Molecular Science and Engineering, Naval Research Laboratory, 4555 Overlook Avenue SW, Washington, D.C. 20375

ABSTRACT The controlled self-assembly of molecules and interactions between them remain a challenge in creating tunable and functional organic nanostructures. One class of molecular systems that has proven useful for incorporating tunable functionality at different length scales is liquid crystals (LCs) due to its ability to inherently self-organize. Here we present a novel approach to utilize the self-assembly of polymerizable liquid crystals to control the molecular aggregation of stable fluorescent chromophores and create a unique class of organic fluorescent nanocolloids. By adjusting the ratio between the dye and LC molecules inside the nanocolloids, we demonstrate the ability to control the molecular interactions and tune the fluorescent emission spectra of nanocolloid populations under single wavelength excitation. The single absorption spectrum and multiple emission spectra are highly desirable and reminiscent of the spectroscopic signature of quantum dots. These novel fluorescent nanocolloids have broad potential applications in fluorescent imaging and biological labeling.

KEYWORDS: liquid crystals · supramolecular assembly · perylene · fluorescent nanocolloids · spectral tuning

The spontaneous molecular order and associated anisotropic properties of liquid crystals (LCs) have been utilized to develop a wide range of nondisplay applications.[1−3] One area of research with vast potential is the confinement of LC molecules within nanocolloids to create nanomaterials with inherent molecular order and/or anisotropic functional properties. Only a handful of published reports have investigated LCs in nanocolloids,[4−7] and these studies probed their stability and demonstrated the ability to incorporate material anisotropy into spherically shaped nanocolloids using either monomeric or lightly cross-linked polymer LCs.[4−6] In addition, Yang *et al.* demonstrated reversible shape changes in nanoparticles composed of high molecular weight main chain LC polymers.[7] Another opportunity that we take advantage of in the current study is the introduction of miscible components into the LC matrix of a nanocolloid to provide multifunctionality.

Here we utilize this concept to mix a highly fluorescent molecule with a polymerizable molecule that exhibits an LC phase to create a set of organic nanocolloids with tuned emission signatures under single wavelength excitation. We demonstrate that the interaction of the LC molecule with the fluorescent dye controls the aggregation number of the fluorescent molecules. The LC component stabilizes the fluorescent molecule in either a monomeric form or a range of stacked assemblies within the nanocolloids. Assembly of the fluorescent dye into dimers, trimers, *etc.* results in a red shift in the fluorescent emission of the nanocolloid populations. By adjusting the ratio between the two molecular species, the $\pi-\pi$ molecular orbital interactions and hence the dye aggregation number tune the fluorescent properties of the nanocolloids. Figure 1 schematically represents the concept where the liquid crystal component acts to segregate the dye molecules in a controlled manner such that the resultant emission signature can be tuned.

The organic chromophore perylene-3,4,9,10-tetracarboxylic diimide was chosen due to its strong absorption and fluorescence, and outstanding chemical, thermal, and photochemical stability.[8,9] It has been shown that perylene tetracarboxylic diimide derivatives in organic solvent possess a concentration-dependent emission signature under single wavelength excitation due to dynamic stacked assemblies maintained through $\pi-\pi$ molecular orbital interactions.[10,11] Red shift in the emission spectrum, observed with increasing dye concentration, was attributed to shifts in the electronic transition from the lowest 0−0 ground state to higher vibronic states, $\nu-\nu'$ (0−1, 0−2, 0−3), as the concentration of the dye was increased.[10,11] We utilize this same aggregation property, but

*Address correspondence to christopher.spillmann@nrl.navy.mil, jawad.naciri@nrl.navy.mil, ratna@nrl.navy.mil.

Received for review July 6, 2009 and accepted September 8, 2009.

Published online September 23, 2009. 10.1021/nn9007498 CCC: $40.75

translate it from an organic solvent to an LC matrix to create stable fluorescent nanocolloid (FNC) populations with tuned emission spectra.

RESULTS AND DISCUSSION

A new perylene derivative, PERC11, was synthesized with two flexible branched alkyl chains terminated by a vinyl group on both sides of the molecule (Figure 2a). The side chains substantially increase the solubility in chloroform as well as decrease the melting point (from 94 to 61 °C) with respect to a perylene homologue without terminal vinyl groups.[12] The absorption and emission characteristics of PERC11 are not affected by the presence of the side chains because of the nodes present at the imide nitrogen in both the HOMO and LUMO $\pi-\pi$ orbitals.[10] These nodes decouple the chromophore properties from the hydrocarbon chains.[13] Following synthesis and purification of PERC11, the material was heated and slowly cooled to observe the optical textures using polarized light microscopy. As shown in Figure 2c, PERC11 shows textures that indicate a higher order mesophase. Discotic mesophases of similar perylene derivatives have been studied previously and show ordered stacking normal to the molecular core.[14] Fluorescence spectroscopy of PERC11 in chloroform revealed a red shift in the emission spectrum as the dye concentration was increased, and the molecules spontaneously aggregate (Supporting Information, Figure S1). This effect is the result of a shift in the vibronic states of the dye aggregate due to the stacking of the $\pi-\pi$ molecular orbitals.[10,11] Nanocolloids containing PERC11 were synthesized using a two-phase miniemulsion process and a final thermal polymerization step.[4−6] This process produces a water suspension of spherical nanocolloids with a range of sizes. Dynamic light scattering (DLS) of the suspensions measured an average hydrodynamic nanocolloid diameter of 150−200 nm with a polydispersity index (PDI) ranging between 0.07 and 0.16, indicating moderate polydispersity. Scanning electron microscopy (SEM) images of nanocolloids deposited on acid-cleaned silicon substrates revealed the nanocolloids to be spherical and confirmed the average diameter. Diameter analysis of the nanocolloid samples from SEM images showed a wide size distribution ranging from 300 to less than 50 nm. SEM images of two samples that represent the polydispersity of the nanocolloids as synthesized are provided in the Supporting Information (Figure S2a,b). Centrifugation was employed to eliminate the smallest and largest nanocolloids and reduce the PDI to a range of 0.05−0.08, indicating nearly monodisperse samples. SEM images confirmed the reduction in the polydispersity of centrifuged samples, most notably by the elimination of nanocolloids less than ~50 nm. Increasing the number of centrifugation steps resulted in further reduction of the nanocolloid diameter range

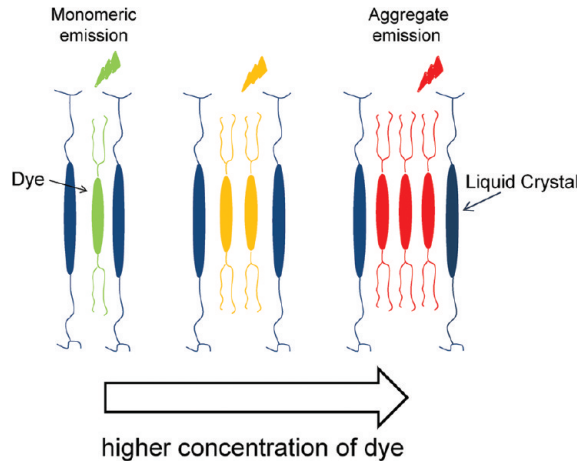

Figure 1. Schematic of dye and cross-linking agent interaction. Control of PERC11 aggregation in FNCs is dictated by the ratio of dye to the nematic cross-linking agent DACTP11. A low ratio of dye to DACTP11 results in a monomeric emission spectrum, while increasing the ratio leads to aggregate formation and a red shift in the emission spectrum.

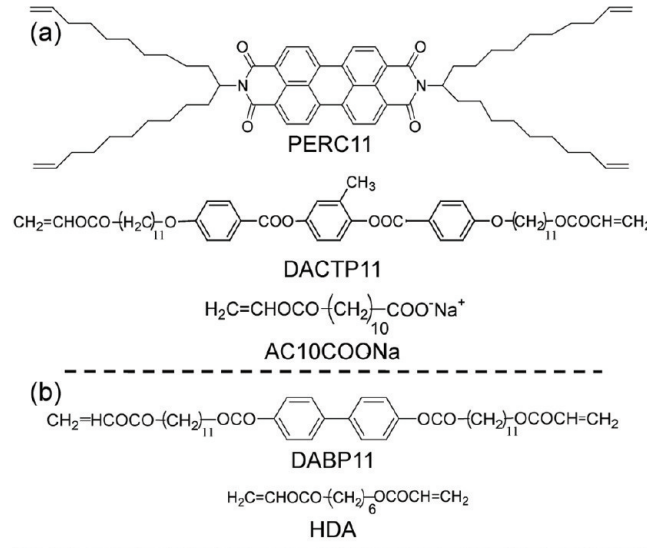

Figure 2. Molecular structures of the components of FNCs. (a) Perylene tetracarboxylate diimide derivative PERC11, liquid crystalline diacrylate cross-linking agent DACTP11 (heating: K 78 N 103 Iso; cooling: K 48 N 103 Iso), and polymerizable carboxylate surfactant AC10COONa. (b) Alternative cross-linking agents DABP11 (K 68 smX 91 Iso) and HDA. (c) Slow cooling of PERC11 to ambient temperature reveals a high order liquid crystalline texture similar to those observed in other perylene derivatives. Scale bar equals 20 μm.

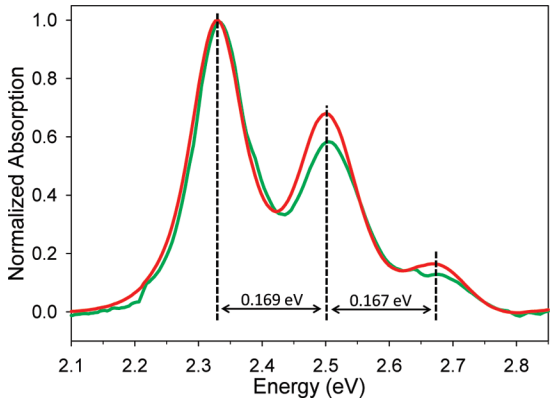

Figure 3. Absorption spectrum of two FNC populations containing 0.6 (green) and 4.8 mol % (red) of PERC11 plotted as a function of energy. Increase in the peak intensities at 2.5 and 2.67 eV is due to a shift from the 0−0 to the 0−1 and 0−2 in the electronic transitions of the PERC11 complexes. Data have been normalized to the highest intensity, and the energy difference between adjacent peaks is indicated.

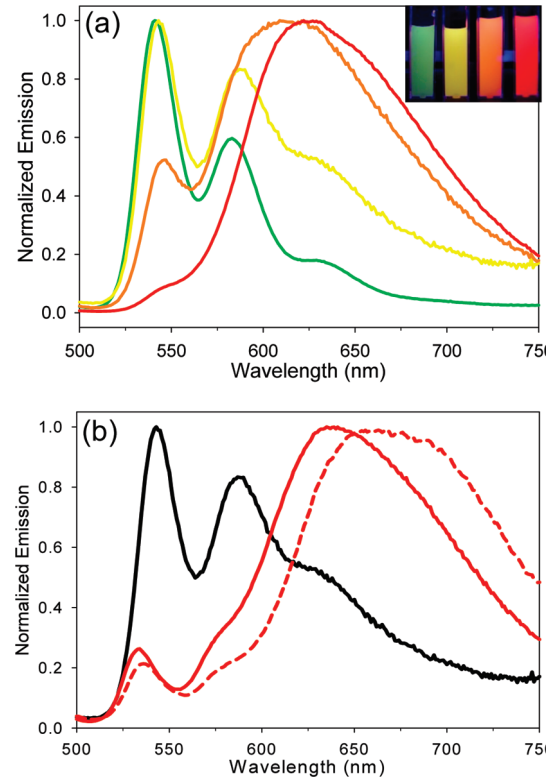

Figure 4. (a) Emission spectra of FNC populations containing 0.6 (green), 1.5 (yellow), 2.5 (orange), and 4.8 (red) mol % of PERC11. Increasing the ratio of PERC11 to DACTP11 in the nanocolloids controllably red shifts the emission spectra. Excitation wavelength for all samples is 488 nm. Inset: Cuvettes of FNC suspensions illuminated under ultraviolet light. (b) Emission spectra of FNCs prepared with 1.54 mol % of PERC11 and cross-linking agent DACTP11 (black), HDA (solid red), or DABP11 (red dashed). Only DACTP11 is able to control the aggregation of PERC11. All spectra have been normalized at their maxima.

from 50 to 300 nm to nearly monodisperse samples (Supporting Information, Figure S2c).

FNCs consisted of the diacrylate cross-linking agent DACTP11, which exhibits a stable LC nematic phase in the monomeric form, and a relatively small proportion of the chromophore PERC11. The mole percentage of dye to cross-linking agent ranged from 0.6 to 4.8%. The polymerizable surfactant with a carboxylate headgroup, AC10COONa (Figure 1a), further stabilized the colloids as has been previously reported.[4] The carboxylic headgroup allows for functionalization of FNC surface, such as conjugation to biomolecules of interest. The end result is FNCs composed of a cross-linked network of LC molecules with well-controlled dye aggregates distributed throughout the interior of the nanocolloid and capped by a functional polymerizable surfactant. Scanning electron micrographs of FNC samples deposited on a silicon substrate reveal well-defined spherical colloids with no indication of particle sintering (Supporting Information, Figure S2). The particles maintain their fluorescence and have been found to be stable for over 12 months.

Comparison of the absorption spectra of FNCs containing 0.6 and 4.8 mol % of PERC11 reveals a distinct increase in the absorption peaks at 2.50 and 2.67 eV with increasing amount of dye (Figure 3). This trend correlates well with our observations made with PERC11 in organic solvent (Supporting Information, Figure S3) and corresponds to a shift from the 0−0 vibronic transition to the 0−1 and 0−2 transitions as isolated monomer PERC11 assembles into oligomers.[10,11] In addition, the energy difference between adjacent peaks is ~0.17 eV, which matches the difference observed in the absorption peaks of PERC11 in organic solvent and agrees with a previous report using a perylene tetracarboxylic derivative.[10] The absorption data of PERC11 in the nanocolloids provide strong evidence that aggregation is being controlled in a manner similar to oligomer formation in organic solvent. The distinct difference in the FNCs is that dye aggregation is not dynamic but has been locked into the nanocolloid population.

Fluorescent spectra of several FNC populations excited at 488 nm show emission signatures dependent upon the amount of dye incorporated into the nanocolloids (Figure 4a). Nanocolloids containing 0.6 mol % of PERC11 exhibit an emission spectrum that mirrors the absorption spectrum, with two predominant peaks at 540 and 580 nm. This spectrum closely matches the monomeric form of PERC11 in organic solvent (Supporting Information, Figure S1). As the ratio of PERC11 to DACTP11 increases, there are two major changes in the emission spectra. First is a general red shift of the emission spectrum, which fits the model where the electronic transitions shift from the lowest vibronic transition state (0−0) to higher states (0−1, 0−2, *etc.*) as the number of dye molecules in the aggregates increase. In addition, there is a change in the shape of the emission spectrum of FNCs with increasing amounts of PERC11. The spectrum of FNCs with 0.6 mol % of PERC11 has a relatively narrow primary emission peak centered at 540 nm. This peak broadens as it shifts to

620 nm when the dye concentration in the nanocolloids increases to 4.8 mol % (Figure 4a). The transformation in the shape of the emission spectra fits with PERC11 aggregate transitions to higher vibronic states accompanied by a loss in resolution of individual peaks. The loss of resolution is well-understood in molecules and aggregates with transitions over a range of energies and is partly due to the surrounding liquid crystal environment that encapsulates the dye.[15] One other notable trend is a significant increase in the energy difference between the first and second emission peaks located at ~2.28 eV (540 nm) and between 2.13 eV (582 nm) and 1.99 eV (623 nm), depending on the dye concentration in the FNCs. When plotted against the amount of dye incorporated into the nanocolloids, the energy shift appears linear (Supporting Information, Figure S4). Taken with the absorption spectra, these data indicate the environment of the PERC11 aggregates embedded in the FNCs is only affecting the emission side of the radiative process. On a Franck−Condon energy diagram, this would equate to a similar absorption transition for all dye concentrations, but a broadening of the excited state potential energy curve upon PERC11 aggregate formation. The energy shift appears to be distinct from crystallochromy,[16,17] where there is a strong dependence of color on the perylene crystal packing, since the surrounding environment of polymerized DACTP11 is constant for all nanocolloid populations.

Confocal images of four different FNC populations deposited on a substrate demonstrate the tuned emission spectra of the FNCs in a dry state (Figure 5a−d). Spectral analysis of individual particles and larger regions of interest reveal that PERC11 aggregates at a given concentration are uniform in an FNC population and independent of nanocolloid size. The emission spectra of the confocal images closely match the emissions observed using fluorescence spectroscopy (compare Figure 5e with Figure 4a).

The interaction between the liquid crystalline cross-linking agent and the dye within the confines of a nanocolloid is a key element to the controlled dye aggregation and spectral tuning of FNCs. To elucidate the role of the LC cross-linking agent, alternative diacrylates were used in place of DACTP11, which exhibits a nematic phase at the temperature used to prepare the nanocolloids. The mole ratio of dye to cross-linking agent was fixed at 1.5%, which produced a yellow fluorescent emission with DACTP11 and indicates a dye assembly between the monomeric (green) and large aggregate (red) forms. At this mole ratio, DACTP11 was first substituted with hexamethylene diacrylate (HDA) (Figure 2b), which is a liquid at room temperature and has no LC phase. HDA has no aromatic core and will not have any π−π molecular orbital interactions with PERC11. Therefore, it was not expected to control the dye aggregation. While stable nanocolloids were synthesized

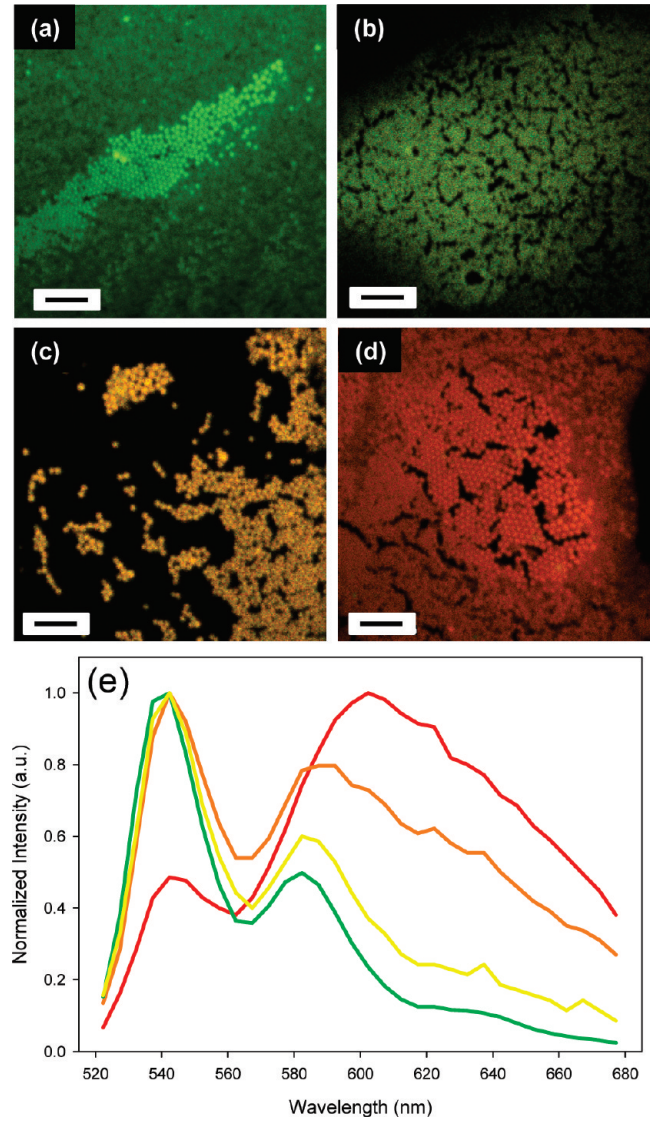

Figure 5. Confocal images of FNC samples deposited and dried on silicon substrate correspond to FNC samples with (a) 0.6, (b) 1.5, (c) 2.5, and (d) 4.8 mol % of PERC11. (e) Average spectral emission of FNCs in images (a−d). Emission curves closely match signature of samples in Figure 4a. Scale bars in each figure equal 2 μm.

with HDA, its inability to control the dye aggregation is demonstrated by the strong red shift in fluorescent emission spectrum (Figure 4b, solid red line).

The second alternative cross-linking agent was DABP11 (Figure 2b), which is a solid at the temperature used to prepare the nanocolloids (64 °C). However, it does have an aromatic core consisting of two phenyl rings and in terms of the molecular aromatic core can be considered an intermediate between HDA and the liquid crystalline DACTP11. When prepared with 1.5 mol % of PERC11, the fluorescent emission was red-shifted compared to the FNCs prepared with DACTP11 (Figure 4b, dashed red line), indicating a high aggregation number of the dye. This observation suggests that the presence of a liquid crystalline phase during synthesis is necessary to control the dye aggregation number. To shed further light on this phenomenon, bulk amounts

of the dye and cross-linking agent were brought into contact with one another to study their miscibility as a function of temperature and time. A preparation of DABP11 and PERC11 revealed that these two components have very low miscibility with limited mixing at the contact line (Supporting Information, Figure S5) at all temperatures. In comparison, a bulk contact preparation of DACTP11 in the nematic phase and PERC11 readily mixed, leading to a broad and diffuse interface between the two components (Supporting Information, Figure S6). The observations of the bulk interactions strengthen the argument that a miscible LC material is required to interact with PERC11 in a manner that is able to control the dye aggregation number and tune the emission spectra of the nanocolloids.

The fluorescent and optical observations indicate that control of PERC11 aggregation in FNCs is driven by three parameters. The first is miscibility of the molecular species in the temperature range used to synthesize the nanocolloids. Immiscibility promotes PERC11 aggregation during FNC synthesis despite encapsulation of both hydrophobic components within the nanocolloid. The second parameter is $\pi-\pi$ molecular interactions between the molecules. HDA is miscible with PERC11 yet offers no influence over the core interactions of PERC11. DABP11 exhibits an LC phase and has an aromatic core but was not miscible with PERC11 to provide sufficient $\pi-\pi$ interactions to control dye aggregation. On the other hand, the nematic DACTP11 is both miscible with PERC11 and has sufficient core interaction to segregate the dye and control aggregation. This indicates that an LC component, specifically a molecule with the necessary core−core interactions with perylene, plays a crucial role in controlling the aggregation of dye molecules. The third parameter necessary to control the dye aggregation is the ratio of the molecular species. By adjusting the mole ratio of PERC11 relative to DACTP11 from 0.6 to nearly 5 mol %, we demonstrate the ability to carefully control the dye aggregation and tune the emission spectra of FNCs over a broad range of the visible spectrum.

To demonstrate the functionality of FNCs, we have bioconjugated the surface using established EDC chemistry to couple the primary amines of NeutrAvidin (NA) to the carboxylate groups on the surface of FNCs. The FNC−NA complexes were then used as fluorescent tracers in a fluid array immunoassay to detect the highly toxic protein ricin. Assay results were compared to those obtained using a standard label, streptavidin−phycoerythrin (SA−PE). A schematic setup of the FNC preparation and assay is shown in Figure 6a. The nanocolloids match the fluorescent intensity obtained by the SA−PE (Figure 6b). In addition, the utility of using nanoparticles as a scaffold to amplify the assay was demonstrated by the subsequent addition of biotinylated PE (Bt-PE), which upon binding to the unoccupied NA on the nanocolloids resulted in a 4-fold increase in fluorescent intensity. These encouraging initial results portend the usefulness of FNCs in a wide range of fluorescent bioassays.

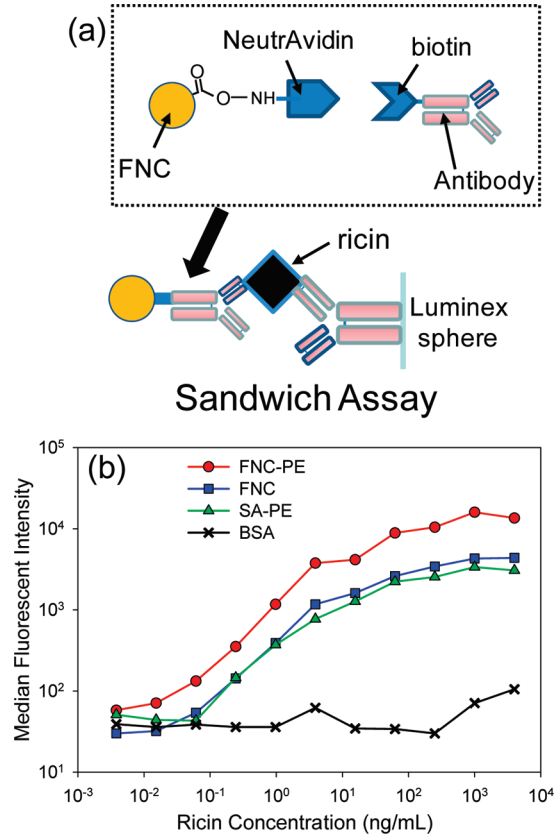

Figure 6. Fluid array immunoassay with FNCs. (a) Schematic representation of FNC−NA coupling to biotinylated anti-ricin antibody to complete a sandwich immunoassay. (b) Intensity of FNC−NA conjugated to anti-ricin antibodies tracked as function of ricin concentration. FNC−NAs (blue) matched signal strength of standard strepavidin−phycoerthrin (SA−PE) bound to anti-ricin (green). Fluorescent intensity of FNC−NAs amplified by addition of biotinylated phycoerythrin (FNC−PE) to NeutrAvidin on nanocolloid surface (red). Microspheres coated with bovine serum albumin (BSA) were included as control for nonspecific binding in each trial, and an example result is shown (black).

Given the intense fluorescence of nanocolloids and their usefulness in fluorescent assays, it is of interest to determine the quantum yield (ϕ) of the FNCs containing varying amounts of perylene. The quantum yield of monomeric perylene derivatives in organic solvent has been reported to be ~1.[18,19] Synthesis of dimeric and trimeric forms of perylene or dynamic dye assemblies in organic solvents causes a red shift in the fluorescence emission and a decrease in ϕ.[11,18] In our system, the dye is confined and distributed in nanocolloids which are suspended in an aqueous medium. The established comparative method described by Williams *et al.* was used to determine the quantum efficiency of the nanocolloids (see Methods for details).[20] The basic approach was to quantify the relationship between the optical density (OD) at a given wavelength and the integrated fluorescent intensity excited at that same wavelength. The re-

sult was then compared to the ϕ of rhodamine 6G in water,[21] which was used as a standard due to similar absorption and fluorescent emission characteristics. Over the range of FNCs studied, the quantum efficiency varied from ~1.0 to 0.6 as the emission spectra shifted from green to red, respectively. For example, the FNC population containing 1.5 mol % of PERC11 had $\phi = 1.02 \pm 0.06$, while the FNCs with 4.8 mol % of PERC11 had $\phi = 0.60 \pm 0.03$. Thus, the quantum yield of the FNCs follows a trend similar to what has been observed with perylene in solution as a function of the aggregation number.

In conclusion, we have transferred the concentration-dependent spectral tuning of perylene from a liquid phase system to a nanocolloid system. The driving force for the formation of FNCs is the manipulation of $\pi-\pi$ molecular orbital interactions in the presence of a second molecular species to control the dye stacking. The molecular structure of the LC cross-linking agent and its phase behavior play a critical role in controlling the perylene molecular aggregates. The organic nanocolloids are highly fluorescent, exhibit a long shelf life, and are easy to bioconjugate, thus overcoming many of the hurdles currently facing quantum dots. This concept can be extended to other perylene derivatives to extend the color range of the nanocolloids. The simplicity of the synthetic approach and ease of surface functionalization opens great opportunity toward the design of other novel multifunctional nanocolloids beyond the FNCs described here.

METHODS

Synthesis. *N,N′*-Bis(1-dec-9-enylundec-10-enyl)perylene-3,4,9,10-tetracarboxylbisimide (PERC11) was synthesized by standard methods.[22] Briefly, perylene-3,4,9,10-tetracarboxyldianhydride was reacted with 1-dec-9-enylundec-10-enylamine, which was synthesized according to Feiler *et al.*,[23] in the presence of zinc acetate dihydrate and imidizale at 180 °C. The final product was purified by column chromatography on silica gel. The synthesis of the polymerizable surfactant AC10COONa and the nematic cross-linking agent DACTP11 has been reported previously.[4] Synthesis of the cross-linking agent DABP11 followed procedures similar to DACTP11, and HDA was purchased from Aldrich and used as received.

Sample Preparations and Experiments. All fluorescent nanocolloid samples were prepared using a two-phase miniemulsion procedure previously described.[4−6] In brief, a diacrylate cross-linking agent, PERC11, and a thermal initiator are dissolved in chloroform (not miscible with water) and added to an aqueous solution containing 15 mg of the surfactant AC10COONa. The total mass of dye and cross-linking material was ~80 mg, the mol % of PERC11 ranged from 0.6 to 4.8 mol %. Stirring and ultrasonication of the mixture produces a stable miniemulsion containing small droplets of the organic materials surrounded by polymerizable surfactant. Upon heating to 64 °C, both the cross-linking agent and surfactant polymerize as the organic solvent slowly evaporates, leaving a nanoparticle suspension stabilized by surfactant. The polymerizable surfactant covalently binds to the cross-linking agents, providing a distinct advantage over conventional surfactants that are physically adsorbed and can result in loss of emulsion stability.

Size and Shape Characterization. Following thermal polymerization, the average diameter and polydispersity index (PDI) of nanocolloid suspensions were quantified using dynamic light scattering (DLS, ZetaPALS zeta potential analyzer, Brookhaven Instruments Corp., Holtsville, NY). Visualization of the shape and diameter of nanocolloids was performed using scanning electron microscopy (SEM) of samples deposited on acid-cleaned Si substrates by vertical pulling from a diluted nanocolloid suspension at a withdrawal rate of 250 nm/s. Diameter analysis of the nanocolloids from SEM images was performed using ImageJ (http://rsbweb.nih.gov/ij/) and involved application of a threshold value to the images followed by a watershed algorithm. The diameter distribution was output by ImageJ.

The polydispersity of the nanocolloid suspensions was significantly reduced by removing the largest and smallest colloids using centrifugation (Eppendorf Centrifuge 5415R, Westbury, NY). Low speed centrifugation at a relative centrifugal force (rcf) of 2000 was first employed to settle the largest particles into a pellet at the bottom of the centrifugation tube. The supernatant was removed, and high speed centrifugation at 8000 rcf was then used to separate the smallest particles, which remained suspended in the supernatant and were discarded. The average nanocolloid diameter remained the same following multiple cycles of this centrifugation approach, and DLS revealed the PDI was lowered to levels that indicate nearly monodisperse samples. This was confirmed by diameter analysis of nanocolloids from SEM images.

Absorption and Fluorescent Characterization. Absorption and fluorescent spectra of diluted FNC suspensions were collected on an HP8453 diode array UV−vis spectrophotometer (Hewlett-Packard) and a FluoroMax-3 spectrofluorometer (Horiba Jobin Yvon), respectively. Confocal images and spectra of nanocolloids deposited on acid-cleaned silicon substrates were collected on a Nikon Eclipse C1si confocal microscope system using 488 nm excitation. The imaging system allows the fluorescent emission spectrum of a sample to be collected over a user-defined region of interest and range of wavelengths.

Quantum Yield. The quantum yield, ϕ, of the nanocolloids was determined using the comparative method of Williams *et al.*[20] and is given as

$$\phi = \phi_R\left(\frac{G}{G_R}\right)\left(\frac{n^2}{n_R^2}\right)$$

where ϕ_R is the quantum efficiency of the fluorescent reference, G is the gradient of the sample integrated fluorescence intensity *versus* the optical density, G_R is the gradient of the fluorescence standard, and n and n_R are the refractive index of the solvent of the sample and fluorescent reference, respectively. Rhodamine 6G was chosen as the fluorescent standard ($\phi_R = 0.95$) due to its similar absorption and emission characteristics to perylene and the fact that the quantum yield was determined at an excitation wavelength of 488 nm (the same excitation used for the FNCs) in an aqueous medium. Because both the standard and the FNCs are suspended in an aqueous medium, $n = n_R$. To calculate the gradient for rhodamine 6G and FNCs, the optical density and the fluorescence spectra at 488 nm excitation were collected in a 10 mm quartz cuvette over a range of dilutions where the maximum OD was less than 0.1. Low OD values were used to avoid nonlinear effects in the relationship between the OD and integrated fluorescent intensity. Baseline corrections were applied to both the absorption and fluorescent data sets. The gradients G and G_R were then determined by linear regression of the OD at 488 nm *versus* the total integrated fluorescent intensity at 488 nm excitation.

Bulk Contact Preparations of PERC11 and Cross-Linking Agents. The miscibility of the dye, PERC11, with the two cross-linking agents DACTP11 and DABP11 was examined using a contact preparation technique with a Linkam hot stage (LTS 350, Linkam Scientific Instruments, Ltd., Surrey, UK) mounted on a polarized light microscope. Cross-linking agent was drawn under a glass coverslip on a microscope slide by capillary action as the sample was

heated to the isotropic phase. When a significant portion of the coverslip area was filled with the cross-linking agent, the sample was cooled and excess material removed. On the opposite side of the preparation, PERC11 was drawn under the coverslip in a similar manner. As the PERC11 approached the cross-linking agent, the temperature of the microscope slide was adjusted to observe the interaction with DACTP11 or DABP11. The mixing at the contact line was then observed as a function of time and/or temperature.

Bioconjugation and Sandwich Assay. For the immunoassay, the carboxylate-terminated surfactant AC10COONa was used to bioconjugate FNCs containing 1.5 mol % of the perylene dye. A standard two-step carbodiimide methodology was used to activate FNCs while in dialysis (10 mM sodium phosphate pH 6.0). The reactants, 1 mg/mL 1-ethyl-3-(3-dimethylaminopropyl) carbodiimide hydrochloride (EDC) and *N*-hydroxysulfosuccinimide (NHS), were added to the FNCs in the dialysis bag. Excess EDC and NHS was removed during the surface activation step to minimize unwanted cross reactions during protein conjugation. After 1 h, an excess (0.5 mg) of NeutrAvidin (NA) was add to FNCs (FNC−NA). The sample was dialyzed overnight in PBS. Unbound NA was removed by centrifugation washing. The FNC−NA complex was resuspended in PBS with 0.05% Tween 20. Dynamic light scattering of the nanocolloids before and after the labeling procedure revealed an increase in the average hydrodynamic diameter from 150 to 168 nm and a small increase in the PDI from 0.05 to 0.08. Throughout the labeling procedure and immunoassay, there was no observation of FNC aggregation. The protocol for the sandwich assay follows. Luminex microspheres (Luminex Corp.) were coated with llama anti-ricin IgG. These microspheres and a control set coated with bovine serum albumin (BSA) were incubated with various concentrations of the highly toxic protein ricin. Unbound ricin was removed by filtration, and the microspheres were then incubated in biotinylated llama anti-ricin IgG. Unbound recognition antibody was also removed *via* filtration, after which the microspheres were incubated in a 50 μL volume with various fluorescent tracers. All incubation times were 30 min. FNC−NA (~6000/μL) was compared to the commercial standard tracer streptavidin−phycoerthrin (SA−PE) at 5 μg/mL. For the FNC−NA sample, signal amplification was also demonstrated by the subsequent addition of biotinylated PE (5 μg/mL) to the FNC−NA surface (FNC−PE), which bound to unoccupied NA on the nanocolloids. In each case, excess tracers were removed by filtration prior to measurement of mean fluorescent intensity with a Luminex 100 (Luminex Corp.).

Acknowledgment. The authors thank the Office of Naval Research (ONR) and the Defense Threat Reduction Agency (DTRA) for financial support. The authors also thank J. Zhou and M. Moore for collecting the absorption spectra of the dye in organic solvent and synthesis of the cross-linking agent DACTP11, respectively.

Supporting Information Available: Figures of the absorption and fluorescent emission of PERC11 in organic solvent, SEM images showing nanocolloid size distribution and shape, description of energy shift in FNC emission spectra, and light microscopy images of bulk contact experiments between dye and cross-linking agents. This material is available free of charge *via* the Internet at http://pubs.acs.org.

REFERENCES AND NOTES

1. Ford, A. D.; Morris, S. M.; Coles, H. J. Phototonics and Lasing in Liquid Crystals. *Mater. Today* **2006**, *9*, 36–42.
2. Woltman, S. J.; Jay, G. D.; Crawford, G. P. Liquid-Crystal Materials Find a New Order in Biomedical Applications. *Nat. Mater.* **2007**, *6*, 929–938.
3. Nie, Z. H.; Kumacheva, E. Patterning Surfaces with Functional Polymers. *Nat. Mater.* **2008**, *7*, 277–290.
4. Spillmann, C. M.; Naciri, J.; Wahl, K. J.; Garner, Y. H.; Chen, M.-S.; Ratna, B. R. Role of Surfactant in the Stability of Liquid Crystal-Based Nanocolloids. *Langmuir* **2009**, *25*, 2419–2426.
5. Tongcher, O.; Sigel, R.; Landfester, K. Liquid Crystal Nanoparticles Prepared as Miniemulsions. *Langmuir* **2006**, *22*, 4504–4511.
6. Vennes, M.; Zentel, R.; Rossle, M.; Stepputat, M.; Kolb, U. Smectic Liquid-Crystalline Colloids by Miniemulsion Techniques. *Adv. Mater.* **2005**, *17*, 2123–2127.
7. Yang, Z. Q.; Huck, W. T. S.; Clarke, S. M.; Tajbakhsh, A. R.; Terentjev, E. M. Shape-Memory Nanoparticles from Inherently Non-spherical Polymer Colloids. *Nat. Mater.* **2005**, *4*, 486–490.
8. Christie, R. M. Pigments, Dyes and Fluorescent Brightening Agents for Plastics—An Overview. *Polym. Int.* **1994**, *34*, 351–361.
9. Nagao, Y.; Misono, T. Synthesis and Properties of *N*-Alkyl-*N*′-aryl-3,4−9,10-perylenebis(bicarboximide). *Dyes Pigm.* **1984**, *5*, 171–188.
10. Wang, W.; Han, J. J.; Wang, L. Q.; Li, L. S.; Shaw, W. J.; Li, A. D. Q. Dynamic π−π Stacked Molecular Assemblies Emit from Green to Red Colors. *Nano Lett.* **2003**, *3*, 455–458.
11. Balakrishnan, K.; Datar, A.; Naddo, T.; Huang, J. L.; Oitker, R.; Yen, M.; Zhao, J. C.; Zang, L. Effect of Side-Chain Substituents on Self-Assembly of Perylene Diimide Molecules: Morphology Control. *J. Am. Chem. Soc.* **2006**, *128*, 7390–7398.
12. Langhals, H.; Demmig, S.; Potrawa, T. The Relation between Packing Effects and Solid-State Fluorescence of Dyes. *J. Prakt. Chem.* **1991**, *333*, 733–748.
13. Wurthner, F. Perylene Bisimide Dyes as Versatile Building Blocks for Functional Supramolecular Architectures. *Chem. Commun.* **2004**, *14*, 1564–1579.
14. Pisula, W.; Kastler, M.; Wasserfallen, D.; Robertson, J. W. F.; Nolde, F.; Kohl, C.; Mullen, K. Pronounced Supramolecular Order in Discotic Donor−Acceptor Mixtures. *Angew. Chem., Int. Ed.* **2006**, *45*, 819–823.
15. Turro, N. J. *Modern Molecular Photochemistry*; University Science Books: Mill Valley, CA, 1991.
16. Kazmaier, P. M.; Hoffmann, R. A Theoretical Study of Crystallochromy. Quantum Interference Effects in the Spectra of Perylene Pigments. *J. Am. Chem. Soc.* **1994**, *116*, 9684–9691.
17. Klebe, G.; Graser, F.; Hadicke, E.; Berndt, J. Crystallochromy as a Solid-State Effect. Correlation of Molecular-Conformation, Crystal Packing and Color in Perylene-3,4-9,10-Bis(Dicarboximide) Pigments. *Acta Crystallogr., Sect. B* **1989**, *45*, 69–77.
18. Giaimo, J. M.; Lockard, J. V.; Sinks, L. E.; Scott, A. M.; Wilson, T. M.; Wasielewski, M. R. Excited Singlet States of Covalently Bound, Cofacial Dimers and Trimers of Perylene-3,4:9,10-bis(dicarboximide)s. *J. Phys. Chem. A* **2008**, *112*, 2322–2330.
19. Kalinin, S.; Speckbacher, M.; Langhals, H.; Johansson, L. B. A. a New and Versatile Fluorescence Standard for Quantum Yield Determination. *Phys. Chem. Chem. Phys.* **2001**, *3*, 172–174.
20. Williams, A. T. R.; Winfield, S. A.; Miller, J. N. Relative Fluorescence Quantum Yields Using a Computer-Controlled Luminescence Spectrometer. *Analyst* **1983**, *108*, 1067–1071.
21. Magde, D.; Rojas, G. E.; Seybold, P. G. Solvent Dependence of the Fluorescence Lifetimes of Xanthene Dyes. *Photochem. Photobiol.* **1999**, *70*, 737–744.
22. Feiler, L.; Langhals, H.; Polborn, K. Synthesis of Perylene-3,4-Dicarboximides—Novel Highly Photostable Fluorescent Dyes. *Liebigs Ann.* **1995**, 1229–1244.
23. Hopkins, T. E.; Wagener, K. B. Amino Acid and Dipeptide Functionalized Polyolefins. *Macromolecules* **2003**, *36*, 2206–2214.